The effect of monovalent anion species on the aggregation and charging of allophane clay nanoparticles

Chihiro Takeshita [a], Kotaro Masuda [a], Motoyoshi Kobayashi [b]

[a] Graduate School of Life and Environmental Sciences, University of Tsukuba, 1-1-1 Tennodai, Tsukuba, Ibaraki 305-8572, Japan

[b] Faculty of Life and Environmental Sciences, University of Tsukuba, 1-1-1 Tennodai, Tsukuba, Ibaraki 305-8572, Japan

Corresponding author: Motoyoshi Kobayashi

Email: kobayashi.moto.fp@u.tsukuba.ac.jp

Conflict of interest

The authors declare that they have no conflict of interest associated with this article.

16   **Abstract**

17   Allophane is a kind of clay mineral which has amorphous hollow spherical structure. To clarify the dispersion,

18   aggregation and charging behaviour of allophane in the presence of various monovalent anions, F^-, Cl^-, Br^-, I^-,

19   BrO_3^-, IO_3^-, and SCN^-, the stability ratio and electrophoretic mobility of allophane were investigated. The

20   stability ratio was obtained from the temporal change in the average hydrodynamic diameter of allophane

21   measured by dynamic light scattering. The charging behaviour was evaluated from the measurement of

22   electrophoretic mobility (EPM) of allophane. These experiments were performed as a function of electrolyte

23   concentration at pH 5, where the net charge of allophane is positive. The experimental results demonstrated

24   that the stability ratio decreased with increasing the salt concentration and finally it became unity independent

25   of the salt concentration. Consequently, we observed slow aggregation regime, fast aggregation regime, and

26   critical coagulation concentration (CCC). Therefore, the stability ratio follow the classical theory of Derjaguin,

27   Landau, Verwey, Overbeek (DLVO) at least qualitatively. However, the CCC of allophane showed difference

28   for each anion species; the CCC followed the order $F^- < IO_3^- < Cl^- < SCN^- < BrO_3^- < Br^- < I^-$. We also confirmed

29   the difference in EPM among anion species; the reduction of EPM magnitude was significant for well-hydrated

30   ions. We presume that the CCC and EPM of allophane depend on the affinity of anions to the allophane surface

31   characterized by the degree of hydration of each ion. That is, well-hydrated anions can adsorb to the

32   hydrophilic surface of allophane and effectively decrease the positive charge of allophane. Besides this, the

33   fluoride ion induced much lower CCC and charge reversal. These results are due to the strong affinity of

34   fluoride ion for the allophane surface. Meanwhile the dependence of CCC on the zeta potential followed the

35   DLVO prediction. Although the zeta potential of allophane is affected by anion species, the CCC behaviors

36   can be understood by the DLVO theory through the evaluation of zeta potential of allophane. This means that

37   the measurement of stability ratio and electrophoretic mobility accompanied with the DLVO theory are

38   valuable tools for the understanding of the aggregation-dispersion of charge-stabilized natural clays.

39

40   **keywords**:   Stability ratio; Dynamic light scattering; Electrophoretic mobility; Critical coagulation

41   concentration; Ion specificity; Hydration

1 Introduction

To understand the dispersion and aggregation behaviors of soil colloids such as clay particles and humic substances is important not only in soil science but also in considering environmental problems [1,2,3,4,5]. Typical clay minerals in young volcanic ash soil are allophane and imogolite. It is thus valuable to understand the aggregation and dispersion of allophane and imogolite when considering the environmental problems in young volcanic ash soils.

Allophane and imogolite are alumino-silicates and have unique features. Allophane is an amorphous hollow spherical particle with an outer diameter of 3-5 nm and the thickness of its wall is about 0.6-1.0 nm [6,7,8]. SiO_2/Al_2O_3 ratio of allophane is reported to vary between 1.0 and 2.0 [7]. The outer and inner surface of the hollow sphere are alumina-like and silica-like, respectively. The aggregation of allophane occurs around its isoelectric point around pH 6-7 [9]. Generally, allophane particles in aquatic suspension exist as irreversible aggregates with diameters of 100-500 nm determined by electron microscopy and particle size measurement in water (Fig. 1). Meanwhile, imogolite has nano-tubular shape and positive zeta potential over a wide range of pH; the isoelectric point of imogolite is over 9 [10]. Classical sedimentation experiments revealed that the imogolite aggregates at pH > 6 [11]. On the one hand, the allophane aggregates only around its isoelectric point around pH 6 [9,11,12]. Although imogolite has larger external surface area than allophane, the amount of reactive AlOH is less than allophane because of fewer defect edge sites on imogolite as compared with allophane [13,14]. These features imply that the charging and aggregation of allophane are more sensitive to the change in solution chemistry. Therefore, this study has focused on the aggregation and charging of allophane.

3

The dispersion-aggregation of colloidal particles has been discussed on the basis of the Derjaguin-Landau-Verwey-Overbeek (DLVO) theory. The DLVO theory claims that the interaction potential energy between two charged particles are given by the sum of electric double layer potential and the van der Waals potential. According to the DLVO theory, the aggregation of colloidal particles is induced by the increased electrolyte concentration and/or the reduced surface electric potential. As a result, with increasing the electrolyte concentration, the rate of aggregation increases in so-called slow aggregation regime and reaches to a constant maximum in so-called fast aggregation regime. The critical coagulation concentration (CCC) is defined as the boundary between these two regimes. It is widely accepted that the DLVO theory suggests that CCC depends on the ionic valence in electrolyte solutions. The DLVO theory has explained the aggregation and dispersion of many natural and synthetic colloidal particles, except for silica nanoparticles and imogolite [12,15,16,17,18,19,20,21].

Systematic studies on the aggregation-dispersion of colloidal particles have demonstrated that the CCC is affected by not only ionic valence but also ionic species. Such effect of ionic species is known as Hofmesister series [22,23,24] and is not considered by the DLVO theory. It is reported that the CCCs of positively charged particles depend on the hydration degree of anions with the same valence [22,23,24]. Nevertheless, the experimental relationship between CCC and surface charge of latex particles follows the DLVO prediction, once the electrokinetically determined surface charge densities, which depend on ion species, are obtained [22].

For the aqueous suspension of allophane particles, specific anion effects on colloidal properties have been

81 studied by measuring the electrophoretic mobility (EPM) and the viscosity of allophane particles and

82 suspension [25,26]. So far, however, systematic simultaneous measurements of the influence of anion species

83 on the aggregation and charging behaviors of allophane are lacking. Therefore, the applicability of the DLVO

84 theory to the aggregation-dispersion of allophane has not been fully examined.

85 To test the applicability of the DLVO theory to the aggregation-dispersion of allophane particles with

86 various types of ions, we have measured the stability ratio of allophane particles with positive charge at pH 5

87 in the presence of various anions with different degree of hydration using dynamic light scattering,

88 accompanied with the measurement of electrophoretic light scattering for the evaluation of zeta potential. The

89 dependence of CCC on the zeta potential at CCC is analyzed on the basis of the DLVO prediction. Such

90 analysis has never been applied to allophane. Therefore, this study provides a novel insight about whether the

91 DLVO works for the aggregation and dispersion of allophane natural clay, once one can evaluate the zeta

92 potential affected by ionic species. Our work can stimulate future researches on the prediction of zeta potential

93 of natural colloidal particles.

94

95 **2   Materials and method**

96 Aggregation and charging behaviors of colloidal/nano particles have been investigated by time-resolved

97 dynamic light scattering and electrophoretic light scattering techniques [9,18,19,20,22,27,28,29,30,31,32,33].

98 Here, we applied these techniques to allophane suspensions with different anion species as a function of the

99 concentration of monovalent electrolyte solution at pH 5, where the net charge of allophane is positive.

100

5

2.1 Materials

The allophane used in this study was purified sample collected from Kitakami pumice, Iwate, Japan. The fine clay fraction (< 0.2 μm) of the pumice grain is allophane-rich [7]. The molar SiO_2/Al_2O_3 ratio of Kitakami allophane is 1.19 [7]. The allophane was obtained and purified by the following method [8,34]. Firstly, we removed gel films of imogolites from the collected pumice. Secondly, the sample was treated with 6 % H_2O_2 solution placed in an oven heated at 110 ° C for 1 hour and left at room temperature for over 15 hours to decompose organic matters. Thirdly, the treated pumice aggregates were squashed and passed through a 0.42 mm sieve, and the H_2O_2 treatment was carried out again. Then, in order to remove small imogolite, the pH of treated suspension was adjusted from 8.5 to 9 using NaOH and sonicated, then the sample was centrifuged. Finally, the suspension of allophane particles with Stokes' diameter below 0.2 μm was collected. At this time, the density of allophane was assumed to be 2.65 g/cm^3 [8]. To saturate the allophane surface with NaCl and to coagulate allophane, NaCl concentration of the allophane suspension was increased to 1 M. This allophane sediment was collected and dialyzed against deionized water until the conductivity of outside solution below 2.0 μS/cm. The allophane was identified by transmission electron microscopy showing the absence of imogolite-like tubes and plate-like clays and pH dependence of electrophoretic mobility and aggregation-sedimentation (Supplementary Information). The isoelectric point (IEP) of the allophane is pH 6-6.5. It should be noted that the IEP of allophane increases with increasing Al/Si ratio [26]. We have not carried out other analyses for the identification. The allophane suspension showed yellow to yellow-brown. Thus the sample contained trace amount of irons.

Sodium salts with various anions, NaF, NaCl, NaBr, NaI, $NaBrO_3$, $NaIO_3$, NaSCN (JIS special grade

121   chemicals, Wako Pure Chemical Industry) were used as electrolytes. HCl solution was used to adjust pH 5.

122   The value of pH after the measurement was checked by a pH meter (B-212, HORIBA). The value of pH was

123   5.13±0.18. All the solutions were filtered through a 0.2 μm syringe filter (DISMIC-25HP). Deionized water

124   was prepared from Elix 5 (Millipore).

125

126   **2.2 Dynamic light scattering**

127   To unveil the effect of anion species on the allophane aggregation, the temporal increase in allophane

128   hydrodynamic diameter d_h in each electrolyte solution was measured as a function of electrolyte

129   concentration by using dynamic light scattering (DLS). The DLS measurements were carried out with

130   Zetasizer Nano (Malvern). In the aggregation experiment, the concentration of allophane was kept 6 mg/L and

131   the pH was adjusted to 5 using HCl solution. All the experiments were performed at 20 ℃.

132   The DLS measurements provide the initial slope of hydrodynamic diameter (dd_h/dt) as a measure of

133   aggregation rate. According to the well-known DLVO theory, the aggregation rate increases with salt

134   concentration and reaches the maximum plateau called a fast aggregation regime, where the electrostatic

135   repulsive force between particles disappears. Meanwhile, at lower salt concentration called a slow aggregation

136   regime, the aggregation is slow because the electric double layer force prevents the aggregation of particles.

137   The aggregation rate is often expressed as the relative aggregation rate so-called stability ratio (W) based on

138   the fast aggregation rate $(dd_h/dt)^f$ [16-24]. Hence, the stability ratio is given by

139     $$W = \frac{(dd_h/dt)^f}{(dd_h/dt)} \qquad\qquad (1)$$

140   where superscript (*f*) refers to a fast aggregation regime [19]. Therefore, as the salt concentration increases,

7

141   the stability ratio decreases, and eventually it becomes unity independent of the salt concentration.

142   From the stability ratio as a function of salt concentration, a critical coagulation concentration (CCC) can

143   be obtained from the boundary concentration between slow aggregation regime and fast aggregation regime.

144   The CCC values can be determined by fitting the experiment data using the following empirical equation:

145    $$\frac{1}{W} = \frac{1}{1+\left(\frac{CCC}{C_s}\right)^{\beta}} \qquad (2)$$

146   where C_s is the concentration of salt and β is the slope dlog $(1/W)$ / dlog (C_s) in the slow aggregation regime

147   [20].

148

149   **2.3 Electrophoretic mobility**

150   To understand the charging behavior of allophane in the presence of various monovalent anions,

151   electrophoretic mobility (EPM) was measured by electrophoretic light scattering with Zetasizer Nano

152   (Malvern). EPM measurements were performed as a function of electrolyte concentration. The allophane

153   concentration was set to 6 mg/L and the pH was adjusted to 5 by the addition of HCl solution if necessary.

154   After mixing the allophane suspension, deionized water, and each electrolyte solution, the mixture was injected

155   into a measurement cell and the mobility measurement was started. From measurements of electrophoretic

156   mobility μ, the zeta or electrokinetic potential ζ is obtained using Smoluchowski's equation as

157    $$\mu = \frac{\varepsilon_0 \varepsilon_r \zeta}{\eta} \qquad (3)$$

158   where ε_0 is the permittivity of vacuum, ε_r is the relative dielectric constant of water, and η is the viscosity

159   of solution. Sophisticated equations including the effect of polarization of electric double layer successfully

160   work for a rigid sphere [35,36]. Nevertheless, such equations are unavailable for the allophane with complex

8

161   structure. Therefore, we obtained the zeta potential at CCC of allophane using Eq. (3). We believe the use of

162   Eq. (3) is reasonable, because the hydrodynamic size is much larger than the Debye length. All the experiments

163   were performed at 20 ℃.

164

3 Result and discussion

3.1 The effect of anion species on the stability ratio of allophane suspension

While the hydrodynamic diameter d_h of allophane in the suspension was constant at low electrolyte concentration, it increased with time t due to aggregation at higher electrolyte concentrations (Fig. 2). The initial slope of dd_h/dt increased with the salt concentration and then reached a constant $(dd_h/dt)^f$. Taking the $(dd_h/dt)^f$ as a reference, we obtained the stability ratio W as $W = (dd_h/dt)^f/(dd_h/dt)$.

The stability ratio of allophane is plotted against the salt concentration in Fig. 3. The symbols denote experimental data obtained from different monovalent anion species. The stability ratio decreases with increasing the salt concentration for any anionic species and becomes unity above the point called critical coagulation concentration (CCC) as shown in Fig. 3. That is, we see clearly the slow aggregation regime, the fast aggregation regime, and the CCC as predicted from the DLVO theory. Therefore, our results of allophane aggregation follow the DLVO theory at least qualitatively. According to the DLVO theory, the electric double layer surrounding the particle develops at a low concentration so that the particles are not able to aggregate. On the one hand, at the high salt concentration, the electric double layer of the particles is compressed, and the particles tend to aggregate due to the van der Waals attraction.

The DLVO theory considers ions as a point charge and thus cannot explain the effect of ion species. Nevertheless, the CCC of allophane depends on the anion types as shown in Fig. 3 and Table 1. The values of CCCs obtained from the experimental value using Eq. (2) are shown in Table 1. The present data show that less hydrated anions result in higher CCC; the CCC follows the order $F^- < IO_3^- < Cl^- < SCN^- < BrO_3^- < Br^- < I^-$. This trend is similar to the result reported by Peula-García et al for positively charged hydrophilic colloidal

10

185   particles, while the opposite tendency was found for hydrophobic latex particles with positive charge [23].

186   Judging from "like" likes "like" rule, we consider that the surface of allophane is rather hydrophilic and

187   positive and thus attracts more well-hydrated anions with larger magnitude of the Gibbs hydration free energy

188   (Table 1), such as F^- and IO_3^- [37].

189   Franks et al. suggested that the IO_3^- ion induces the additional attractive force between alumina particles

190   from the measurement of the yield stress of alumina suspension [38]. Since the outer surface of allophane is

191   alumina-like, one might expect the enhancement of aggregation rate by IO_3^- due to the additional attractive

192   force. Such acceleration of the rate can be seen for the aggregation with larger ionic substances such as polymer

193   and proteins [18,39]. Nevertheless, our data show the minimum stability ratio, based on the fast aggregation

194   at high NaCl concentration, with IO_3^- is unity and thus do not show any symptoms of enhancement of

195   aggregation rate by such strong attractive force in the fast aggregation regime. This is probably due to that the

196   stability ratio is determined by the approaching process, meanwhile the yield stress is governed by the

197   detachment force, which is more sensitive at shorter particle-particle distance [17].

198   To focus more on the effect of the degree of hydration on CCC, we plot the CCC of positively charged

199   colloids obtained from our experiments and literature against the hydration free energy of each anions (-

200     $\Delta hyd G$) in Fig. 4. Although the critical stabilization concentration (CSC), defined as the minimum salt

201   concentration at which the system begins to re-stabilize when salt concentration is increased even more, has

202   been reported for the positively charged hydrophilic colloids, we did not catch such behaviors for allophane

203   particles. Figure 4 indicates that anions with small magnitude of hydration energy (-$\Delta hyd G$), weakly-hydrated

11

204   anions, lead to lower CCC for hydrophobic colloids (Fig. 4b). Conversely, the CCCs of positive hydrophilic

205   colloid and allophane become low for the anions with larger hydration energy, that is, well-hydrated anions

206   (Fig. 4a, b). Again, "like" likes "like" rule helps our understanding. Well/poorly hydrated ions are more likely

207   to adsorb to hydrophilic/hydrophobic particles and reduce the surface charge. Therefore, the water structure

208   around both the particle surface and the hydrated ions influence the CCC tendency. In addition, hydrophobic

209   particles seem to have a constant CCC at the high hydration energy ($-\Delta hyd G$), while allophane shows a

210   constant CCC value at the low hydration energy ($-\Delta hyd G$). The counter-ions with stronger affinity to the

211   surface effectively reduce the surface charge and CCC. Meanwhile, the counter-ions with lower affinity to the

212   surface induce the saturated-like CCCs. This is probably because the main attraction between poorly/well

213   hydrated counter ions and hydrophilic/hydrophobic surfaces is only electrostatic and the ion specificity is

214   negligible. As a consequence, the positive charge of allophone is reduced by the adsorption of well-hydrated

215   anions. The reduction of charge density leads to lower CCC. Such decrease in the surface charge can be

216   inferred from the data of electrophoretic mobility in the section below.

217

218   **3.2 The effect of anion species on electrophoretic mobility of allophane**

219   Figure 5 shows the electrophoretic mobility (EPM) of allophane as a function of salt concentration.

220   Different symbols stand for different monovalent anion species. At the low salt concentration, all the EPM

221   values are positive, demonstrating the positive charge of allophane surface. As the salt concentration increases,

222   the magnitude of EPM decreases because of the compression of electric double layer and the adsorption of

223   counter-ions.

224　　　　Looking into the effect of anion species in Fig. 5, we can confirm the difference in EPM among anion

225　　　　species. The fluoride ion gives rise to a clear charge reversal. The value of EPM shows the order $F^- < IO_3^- <$

226　　　　$BrO_3^- < SCN^- < Cl^- < Br^- < I^-$. We presume that the EPM of allophane is affected by the difference in the degree

227　　　　of hydration of each ion through the change in their affinity to the allophane surface as discussed in the

228　　　　previous section. That is, well-hydrated anions can be accumulated to the hydrophilic surface of allophane and

229　　　　effectively weaken the positive charge of allophane. Thus, the EPM is lower for the well-hydrated ions.

230　　　　The structure of allophane is a hollow sphere with inner silica-like and outer alumina-like surfaces.

231　　　　Therefore, the comparison with previous studies on the anion specific effects on the adsorption and zeta

232　　　　potential of alumina provides useful support to consider the EPM of allophane. The surface of alumina is

233　　　　positively charged at pH below 7-9 [38,40,41]. Szczepaniak and Kościelna measured the adsorption of halogen

234　　　　anions on alumina and showed the adsorption amount followed the order $F^- > IO_3^- > BrO_3^- > Cl^- > Br^- > I^-$ [42].

235　　　　Franks et al. showed that the zeta potential of alumina at low and neutral pH follows the order $Cl^- > BrO_3^- >$

236　　　　IO_3^- [38]. These results are in line with the present data on allophane. The outer surface of allophane with

237　　　　alumina type is likely to be hydrophilic and thus accumulates well-hydrated ions (in other words, structure-

238　　　　making ions [38]), while the detail of the adsorption mechanism is still far from complete.

239　　　　Moreover, in the presence of the fluoride ion, the charge inversion was confirmed. From the results of DLS

240　　　　and EPM, we can conclude that fluoride ion has a much strong affinity with allophane as shown in refs. [26,

241　　　　43, 44]. The strong adsorption of fluoride on allophane is dependent on the types of allophane and is considered

242　　　　to be due to the formation of inner-sphere complex though ligand exchange [26, 43]. The calculation by

243   equilibrium speciation model Visual MINTEQ (https://vminteq.lwr.kth.se/) demonstrates 98.5 % of F is F^- and

244   1.5 % of F is HF at pH 5 around CCC and IEP with NaF. The existence of HF might induce chemical reactions

245   to silicates. According to the study of Su et al. [26], allophane can be transformed to sodium aluminum fluoride

246   (cryolite, Na_3AlF_6) after 24 hr treatment in 0.01 M NaF at a final pH of 4.2. Therefore, the allophane solid

247   phase with fluoride becomes quite different from the original allophane solid phase.

248   Also, iodate can be reduced by the reaction with redox active species. This may result in the decrease in

249   ionic strength. If the reduction of iodate is significant, the CCC and magnitude of EPM should be larger

250   because of the decrease in ionic strength. Nevertheless, our experimental results show the opposite trend. Thus,

251   the reduction effect may not be so important. The decreases in CCC and zeta potential are probably due to

252   relatively stronger adsorption of iodate. Iodate can be adsorbed to alumina by both inner-sphere complex and

253   outer sphere complex and the outer sphere complex dominates at lower pH and lower ionic strength [45]. If

254   this result is applicable to our allophane system, the stronger adsorption of iodate to allophane is partly due to

255   the formation of inner sphere complex.

256

257   **3.3 The relationship between CCC and zeta potential**

258   Our results show that CCC depends on ion species through the change in effective surface charge mediated

259   by the adsorption of the counter-ions with different affinity to the allophane surface. Recently, Trefalt et al.

260   [46] and Oncsik et al. [22] found that the relationship between CCC and surface charge/potential reasonably

261   followed the DLVO prediction for model latex particles, while both the CCC and the surface charge density

262   showed the dependency on ion species. This means that the aggregation and dispersion of charge-stabilized

263   colloid can be discussed on the basis of the DLVO theory, once the surface charge/potential, which is affected

264   by the specificity of ions, is characterized. To confirm the applicability of their idea to allophane, we here

265   compare our CCC vs. zeta potential relation with the prediction by the DLVO theory [22,46].

266   According to the DLVO theory, the interaction energy equation between two particles is shown by

267    $$V = V_{vdW} + V_{DL} \qquad (4)$$

268   where V_{vdW} is the van der Waals interaction energy, and V_{DL} is the double layer overlap energy. The van der

269   Waals interaction energy is given by

270    $$V_{vdW} = -\frac{Ha}{12h} \qquad (5)$$

271   where H is the Hamaker constant for allophane-allophane in water, a is the particle radius, h is the surface

272   separation distance.   The electrostatic repulsive potential between particles at large separation is expressed

273   by

274    $$V_{DL} = 2\pi a \varepsilon_r \varepsilon_0 {\psi_0}^2 \exp(-\kappa h) \qquad (6)$$

275   where ψ_0 is surface potential and κ is given by

276    $$\kappa^2 = \frac{2N_A e^2 I}{\varepsilon_r \varepsilon_0 k_B T} \qquad (7)$$

277   where I is the ionic strength in mol/m^3, N_A is the Avogadro number, and e is the elementary charge.

278   The CCC can be derived by assuming the energy barrier disappears at CCC, namely

279    $$V = 0 \text{ and } \frac{dV}{dh} = 0 \qquad (8)$$

280   Combining these equation, one can get the equation relating CCC and surface potential given by

281    $$CCC = \left(\frac{24\pi\varepsilon_0\varepsilon_r{\psi_0}^2}{\exp(1)H}\right)^2 \cdot \frac{\varepsilon_r\varepsilon_0 k_B T}{2N_A e^2} \qquad (9)$$

15

282   Figure 6 shows the relationship between CCC and zeta/surface potential. The symbols and the solid line

283   denote the experimental values and the DLVO prediction, respectively. The zeta potential, calculated by Eq.

284   (3) the Smolchowski's equation, at CCC is used instead of the surface potential in Eq. (9). We assume the

285   Hamaker constant is 3.5×10^{-20} J, which is reasonable because the allophane is composed of silica and alumina

286   and this value is between silica's one and alumina's one.

287   As shown in Fig. 6, the prediction by DLVO theory is in reasonable agreement with the experimental

288   relationship between CCC and zeta potential. Namely, in terms of CCC, the DLVO theory works for natural

289   clay allophane with rather complicated structure, as found for model latex particles. Our results demonstrate

290   that the measurement of stability ratio and electrophoretic mobility accompanied with the DLVO theory are

291   useful tools for the study of the aggregation-dispersion of charge-stabilized colloids including natural clays.

292   However, it still remains unclear how one can quantitatively predict the effect of ionic species on zeta potential

293   and electrophoretic mobility of natural clays. This point should be unveiled by further studies. In addition,

294   allophanes from different origins have different Si/Al ratios and charging properties. Nevertheless, our result

295   is based on one type of allophane. Therefore, future studies should examine the effect of Si/Al ratio on anion

296   specificity.

4 Conclusion

We measured the stability ratio and electrophoretic mobility (EPM) of allophane at pH 5 as a function of the concentration of sodium salts of different monovalent anions F^-, Cl^-, Br^-, I^-, BrO_3^-, IO_3^-, and SCN^-. Our results of stability ratio showed a difference in critical coagulation concentration (CCC) for each anion. The dependence of EPM of allophane on the salt concentration was also affected by anionic species. The reduction degree of EPM magnitude of allophane in this study was significant for well-hydrated ions, while the opposite trend was demonstrated for hydrophobic latex colloid [22].

We presume that the difference in the degree of hydration of each ion affects the charging behavior of allophane. That is, more strongly hydrated counter-ions are adsorbed on the hydrophilic allophane surface and thus the charge of allophane is effectively decreased. For fluoride ion, much lower CCC and charge inversion detected by EPM were confirmed. These results demonstrate that fluoride ion has strong affinity with allophane. The experimental relationship between CCC and zeta potential follows the prediction by the DLVO theory. Namely, the CCC of allophane varies with the fourth power of the zeta potential. While the zeta potential is influenced by anion species, the CCC behaviors can be explained by DLVO theory, which neglects ion specificity, through the evaluation of zeta potential.

316   **References**

317   [1]   V.P. Evandelou, *Environmental Soil and Water Chemistry: Principles and Applications*. 1998.

318   [2]   B. R. Magee, L. W. Lion, and A. T. Lemley, "Transport of Dissolved Organic Macromolecules and Their Effect

319   on the Transport of Phenanthrene in Porous Media," *Environ. Sci. Technol.*, vol. 25, no. 2, pp. 323–331, 1991.

320   [3]   K. Itami and H. Fujitani, "Charge characteristics and related dispersion/flocculation behavior of soil colloids as

321   the cause of turbidity," *Colloids Surfaces A Physicochem. Eng. Asp.*, vol. 265, no. 1–3, pp. 55–63, 2005.

322   [4]   E. M. Hotze, T. Phenrat, and G. V. Lowry, "Nanoparticle Aggregation: Challenges to Understanding Transport

323   and Reactivity in the Environment," *J. Environ. Qual.*, vol. 39, no. 6, p. 1909, 2010.

324   [5]   P. Christian, F. Von Der Kammer, M. Baalousha, and T. Hofmann, "Nanoparticles: Structure, properties,

325   preparation and behaviour in environmental media," *Ecotoxicology*, vol. 17, no. 5, pp. 326–343, 2008.

326   [6]   M. F. Brigatti, E. Galán, and B. K. G. Theng, "Structure and Mineralogy of Clay Minerals," *Dev. Clay Sci.*, 2013.

327   [7]   T. Henmi and K. Wada, "Morphology and composition of allophane," *Am. Mineral.*, vol. 61, pp. 379–390, 1976.

328   [8]   S. Wada and K. Wada, "Density and structure of allophane," *Clay Miner.*, vol. 12, pp. 289–298, 1977.

329   [9]   Y. Adachi, S. Koga, M. Kobayashi, and M. Inada, "Study of colloidal stability of allophane dispersion by

330   dynamic light scattering," *Colloids Surfaces A Physicochem. Eng. Asp.*, vol. 265, no. 1–3, pp. 149–154, 2005.

331   [10]   J. Karube, K. Nakaishi, H. Sugimoto, and M. Fujihira, "Electrophoretic behavior of imogolite under alkaline

332   conditions," *Clays Clay Miner.*, vol. 40, no. 6, pp. 625–628, 1992.

333   [11]   J. Karube, H. Sugimoto, M. Fujihira, and K. Nakaishi, "Stability and Charge Characteristics of Allophane and

334   Imogolite," *Trans. Japanese Soc. Irrig. Drain. Reclam. Eng.*, vol. 196, no. 66, pp. 103–110, 1998.

335   [12]   M. Kobayashi, M. Nitanai, N. Satta, and Y. Adachi, "Coagulation and charging of latex particles in the presence

336   of imogolite," *Colloids Surfaces A Physicochem. Eng. Asp.*, vol. 435, pp. 139–146, 2013.

337   [13]   C. J. Clark, "Cation and Anion Retention by Natural and Synthetic Allophane and Imogolite," *Clays Clay Miner.*,

338   1984.

339   [14]   B. K. G. Theng, "Surface Properties of Allophane, Halloysite, and Imogolite," *Clays Clay Miner.*, 1982.

340   [15]   E. Tombácz and M. Szekeres, "Colloidal behavior of aqueous montmorillonite suspensions: The specific role of

341   pH in the presence of indifferent electrolytes," *Appl. Clay Sci.*, vol. 27, no. 1–2, pp. 75–94, 2004.

342   [16]   S. H. Behrens, D. I. Christl, R. Emmerzael, P. Schurtenberger, and M. Borkovec, "Charging and Aggregation

343   Properties of Carboxyl Latex Particles: Experiments versus DLVO Theory," *Langmuir*, vol. 16, no. 6, pp.

344   2566–2575, 2000.

345   [17]   M. Kobayashi, S. Yuki, and Y. Adachi, "Effect of anionic surfactants on the stability ratio and electrophoretic

346   mobility of colloidal hematite particles," *Colloids Surfaces A Physicochem. Eng. Asp.*, vol. 510, pp. 190–197,

347   2016.

348   [18]   Y. Huang, A. Yamaguchi, T. D. Pham, and M. Kobayashi, "Charging and aggregation behavior of silica particles

349   in the presence of lysozymes," *Colloid Polym. Sci.*, vol. 296, no. 1, pp. 145–155, 2018.

350   [19]   R. Kretzschmar, H. Holthoff, and H. Sticher, "Influence of pH and humic acid on coagulation kinetics of

351   kaolinite: A dynamic light scattering study," *J. Colloid Interface Sci.*, vol. 202, no. 1, pp. 95–103, 1998.

352   [20]   D. Grolimund, M. Elimelech, and M. Borkovec, "Aggregation and deposition kinetics of mobile colloidal

353   particles in natural porous media," *Colloids and Surfaces A: Physicochemical and Engineering Aspects*, vol. 191,

354   pp. 179-188, 2001..

355   [21]   M. Kobayashi, F. Juillerat, P. Galletto, P. Bowen, and M. Borkovec, "Aggregation and charging of colloidal

356   silica particles: Effect of particle size," *Langmuir*, vol. 21, no. 13, pp. 5761–5769, 2005.

357   [22]   T. Oncsik, G. Trefalt, M. Borkovec, and I. Szilagyi, "Specific ion effects on particle aggregation induced by

358   monovalent salts within the Hofmeister series," *Langmuir*, vol. 31, no. 13, pp. 3799–3807, 2015.

359   [23]   J. M. Peula-García, J. L. Ortega-Vinuesa, and D. Bastos-González, "Inversion of hofmeister series by changing

360   the surface of colloidal particles from hydrophobic to hydrophilic," *J. Phys. Chem. C*, vol. 114, no. 25, pp.

361   11133–11139, 2010.

362   [24]   M. Pavlovic, R. Huber, M. Adok-Sipiczki, C. Nardin, and I. Szilagyi, "Ion specific effects on the stability of

363   layered double hydroxide colloids," *Soft Matter*, vol. 12, no. 17, pp. 4024–4033, 2016.

364   [25]   K. Egashira, "Effect of adsorbed ions on the viscosity of allophane and imogolite clay suspensions," *Clay Sci.*,

365   vol. 5, no. 1, pp. 137–144, 1978.

366   [26]   C. Su and J. B. Harsh, "The electrophoretic mobility of imogolite and allophane in the presence of inorganic

367   anions and citrate," *Clays Clay Miner.*, vol. 41, no. 4, pp. 461–471, 1993.

368   [27]   M. R. Das, J. M. Borah, W. Kunz, B. W. Ninham, and S. Mahiuddin, "Ion specificity of the zeta potential of α-

369   alumina, and of the adsorption of p-hydroxybenzoate at the α-alumina-water interface," *J. Colloid Interface Sci.*,

370   vol. 344, pp. 482–491, 2010.

371   [28]   T. Sugimoto, M. Nishiya, and M. Kobayashi, "Electrophoretic mobility of carboxyl latex particles: effects of

372   hydrophobic monovalent counter-ions," *Colloid Polym. Sci.*, vol. 295, no. 12, pp. 2405–2411, 2017.

20

373 [29] A. Yamaguchi and M. Kobayashi, "Quantitative evaluation of shift of slipping plane and counterion binding to

374 lysozyme by electrophoresis method," *Colloid Polym. Sci.*, vol. 294, no. 6, pp. 1019–1026, 2016.

375 [30] H. Holthoff, S. U. Egelhaaf, M. Borkovec, P. Schurtenberger, and H. Sticher, "Coagulation Rate Measurements

376 of Colloidal Particles by Simultaneous Static and Dynamic Light Scattering," *Langmuir*, vol. 12, no. 23, pp.

377 5541–5549, 1996.

378 [31] B. Jachimska, M. Wasilewska, and Z. Adamczyk, "Characterization of globular protein solutions by dynamic

379 light scattering, electrophoretic mobility, and viscosity measurements," *Langmuir*, vol. 24, no. 13, pp. 6867–

380 6872, 2008.

381 [32] A. Hakim and M. Kobayashi, "Aggregation and charge reversal of humic substances in the presence of

382 hydrophobic monovalent counter-ions: Effect of hydrophobicity of humic substances," *Colloids Surfaces A*

383 *Physicochem. Eng. Asp.*, vol. 540, no. November 2017, pp. 1–10, 2018.

384 [33] S. P. Narvekar, T. Ritschel, and K. U. Totsche, "Colloidal Stability and Mobility of Extracellular Polymeric

385 Substance Amended Hematite Nanoparticles," *Vadose Zone J.*, vol. 16, no. 8, 2017.

386 [34] J. Karube, K. Nakaishi, H. Sugimoto, and M. Fujihira, "Size and shape of allophane particles in dispersed

387 aqueous systems" *Clays and Clay Minerals*, vol. 44, no. 4, pp. 485–491, 1996.

388 [35] T. Sugimoto, M. Kobayashi, and Y. Adachi, "The effect of double layer repulsion on the rate of turbulent and

389 Brownian aggregation: Experimental consideration," *Colloids Surfaces A Physicochem. Eng. Asp.*, vol. 443, pp.

390 418–424, 2014.

391 [36] M. Kobayashi, "Electrophoretic mobility of latex spheres in the presence of divalent ions: Experiments and

392   modeling," *Colloid Polym. Sci.*, vol. 286, no. 8–9, pp. 935–940, 2008.

393   [37]   J. Lyklema, "Simple Hofmeister series," *Chem. Phys. Lett.*, vol. 467, no. 4–6, pp. 217–222, 2009.

394   [38]   G. V. Franks, S. B. Johnson, P. J. Scales, D. V. Boger, and T. W. Healy, "Ion-specific strength of attractive

395   particle networks," *Langmuir*, vol. 15, no. 13, pp. 4411–4420, 1999.

396   [39]   I. Szilagyi, G. Trefalt, A. Tiraferri, P. Maroni, and M. Borkovec, "Polyelectrolyte adsorption, interparticle forces,

397   and colloidal aggregation," *Soft Matter*, vol. 10, no. 15, pp. 2479–2502, 2014.

398   [40]   T. D. Pham, M. Kobayashi, and Y. Adachi, "Interfacial characterization of α-alumina with small surface area by

399   streaming potential and chromatography," *Colloids Surfaces A Physicochem. Eng. Asp.*, vol. 436, pp. 148–157,

400   2013.

401   [41]   M. Kosmulski, "IEP as a parameter characterizing the pH-dependent surface charging of materials other than

402   metal oxides," *Adv. Colloid Interface Sci.*, vol. 171–172, pp. 77–86, 2012.

403   [42]   W. Szczepaniak and H. Kościelna, "Specific adsorption of halogen anions on hydrous γ-Al_2O_3," *Anal. Chim.*

404   *Acta*, vol. 470, no. 2, pp. 263–276, 2002.

405   [43]   S. Kaufhold, R. Dohrmann, Z. Abidin, T. Henmi, N. Matsue, L. Eichinger, A. Kaufhold, and R. Jahn, "Allophane

406   compared with other sorbent minerals for the removal of fluoride from water with particular focus on a mineable

407   Ecuadorian allophane," Applied Clay Science, vol. 50(1), pp. 25-33, 2010.

408   [44]   M. Fieldes and K.W. Perrott, "The nature of allophane in soils. Part 3.," New Zealand Journal of Science, vol. 9,

409   pp. 623-629, 1966.

410   [45]   T. Nagata and K. Fukushi, "Prediction of iodate adsorption and surface speciation on oxides by surface

411   complexation modeling," *Geochimica et Cosmochimica Acta*, vol. 74(21), pp. 6000-6013, 2010.

412   [46]   G. Trefalt, I. Szilagyi, G. Téllez, and M. Borkovec, "Colloidal Stability in Asymmetric Electrolytes:

413   Modifications of the Schulze-Hardy Rule," *Langmuir*, vol. 33, no. 7, pp. 1695–1704, 2017.

414   [47]   Y. Marcus, "A simple empirical model describing the thermodynamics of hydration of ions of widely varying

415   charges, sizes, and shapes," *Biophys. Chem.*, vol. 51, no. 2–3, pp. 111–127, 1994.

416

417

418 **Table 1 Hydration free energy of used anions, and CCC and zeta potential at CCC of allophane** [47]**.**

	F^-	Cl^-	Br^-	I^-	BrO_3^-	IO_3^-	SCN^-
Gibbs free energy of hydration (kJ/mol)[44]	-465	-340	-315	-275	-330	-400	-280
CCC (mmol/L)	0.265	6.75	14.7	16.8	10.6	3.57	8.72
Zeta potential at CCC (mV)	8.37	25.5	26.1	28.5	22.8	20.1	26.9

419

420
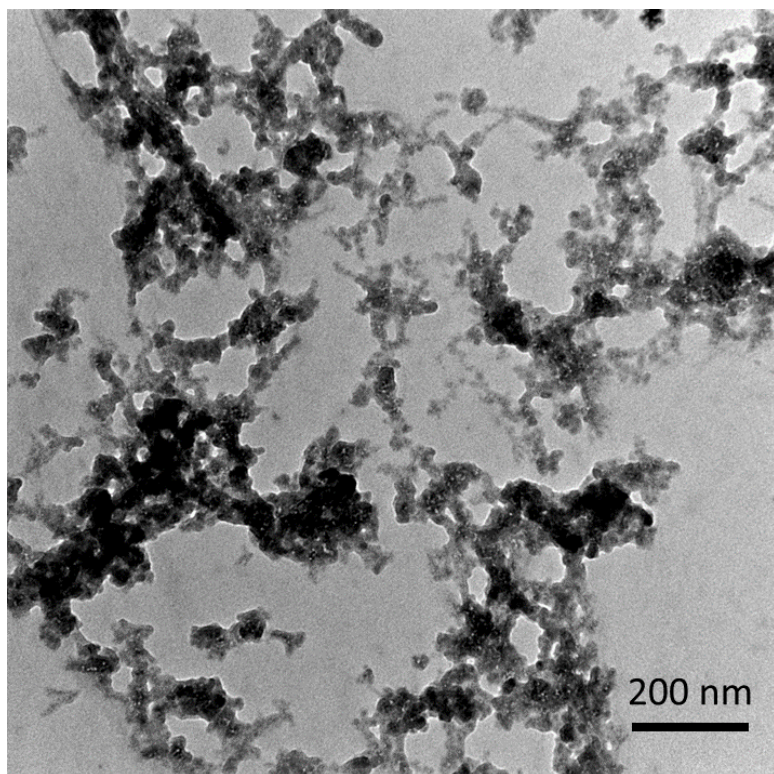
421   **Fig. 1. TEM micrograph of allophane at pH 4.**

422
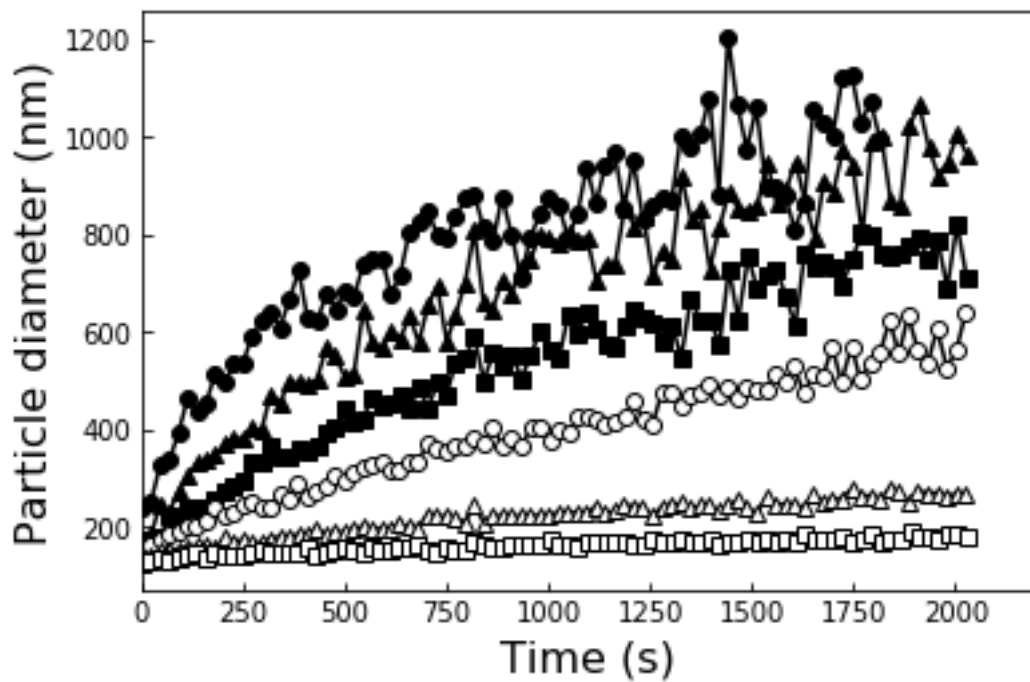
Fig. 2. Hydrodynamic diameter of allophane aggregate as a function of time for different NaCl concentrations at pH 5: 0.1 M (●), 0.008 M (▲), 0.006 M (■), 0.005 M (○), 0.004 M (△), 0.003 M (□).
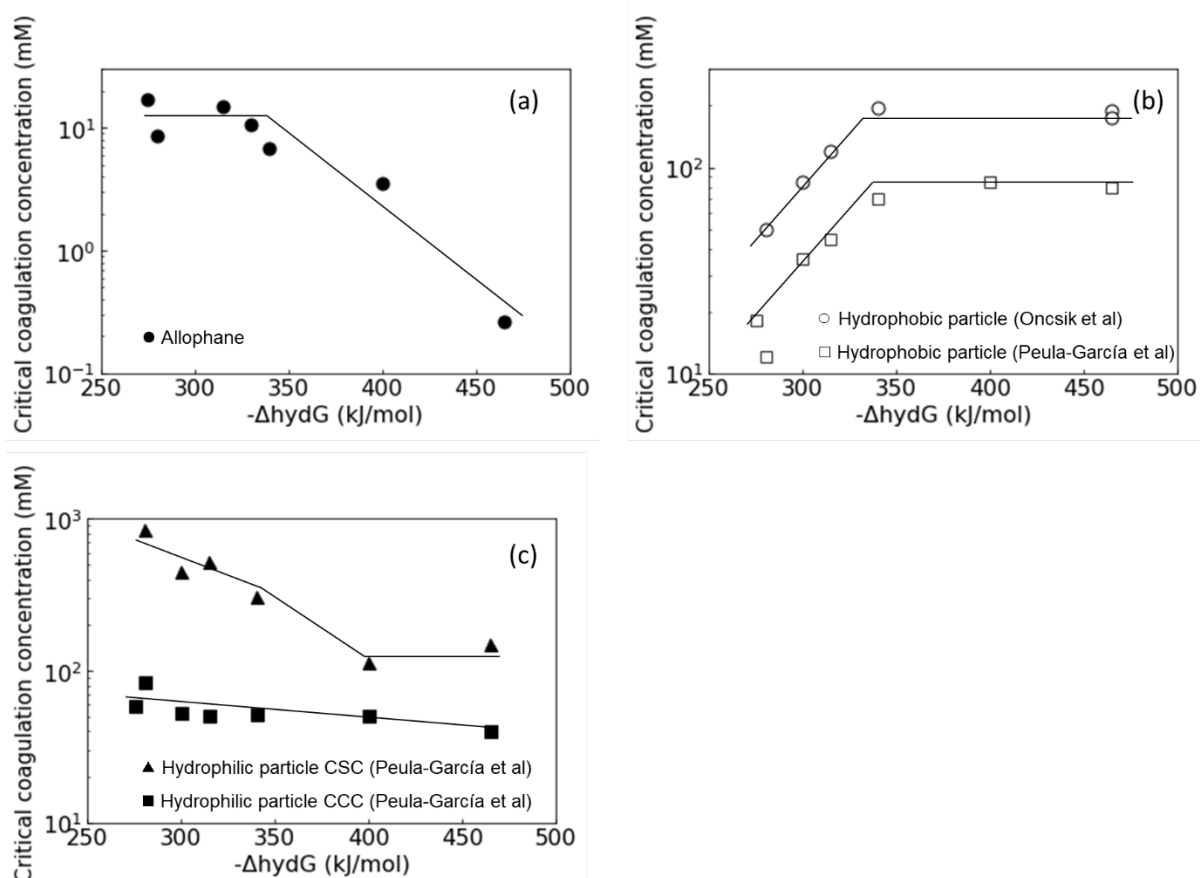
427
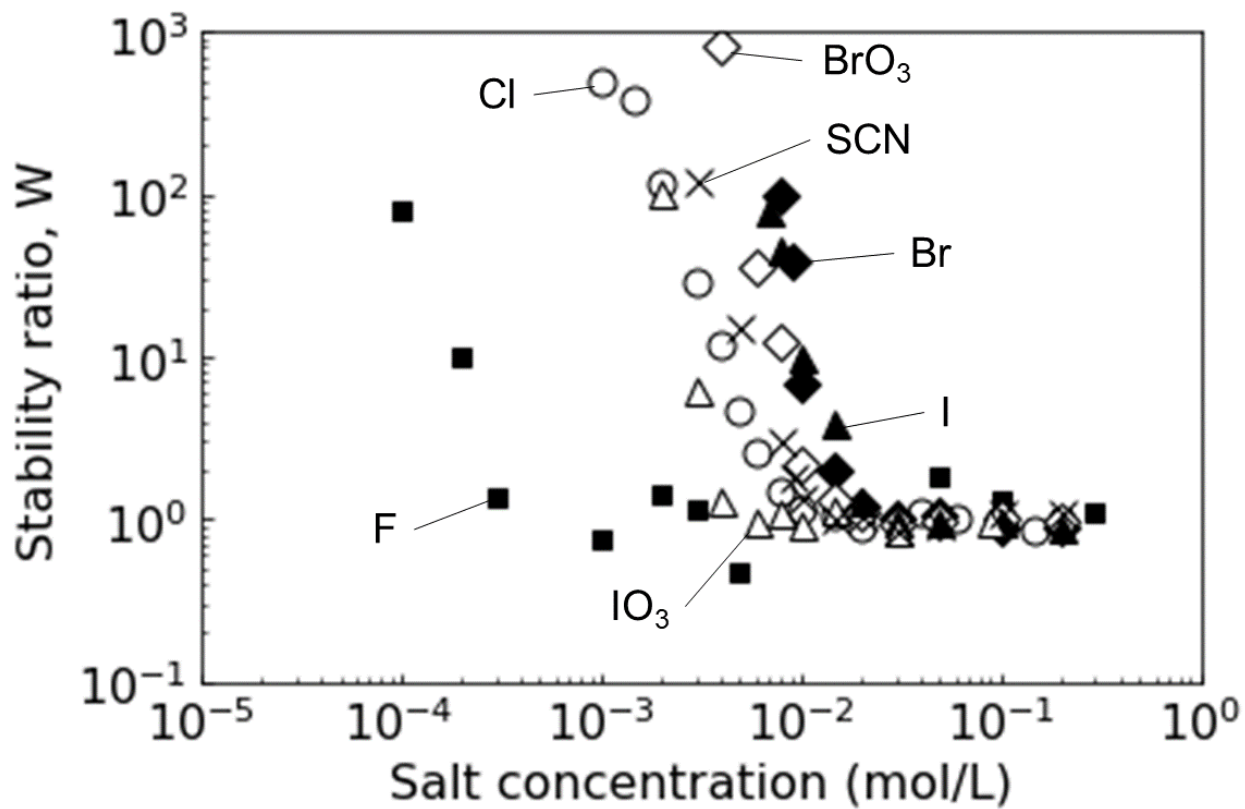
Fig. 3. Stability ratio of allophane as a function of the concentration of various monovalent sodium salts.

The particle concentration was 6 mg/L and the pH was fixed at 5.

430

431

432

433

434 **Fig. 4. (a) Critical coagulation concentrations (CCCs) obtained by the present experiments for the**
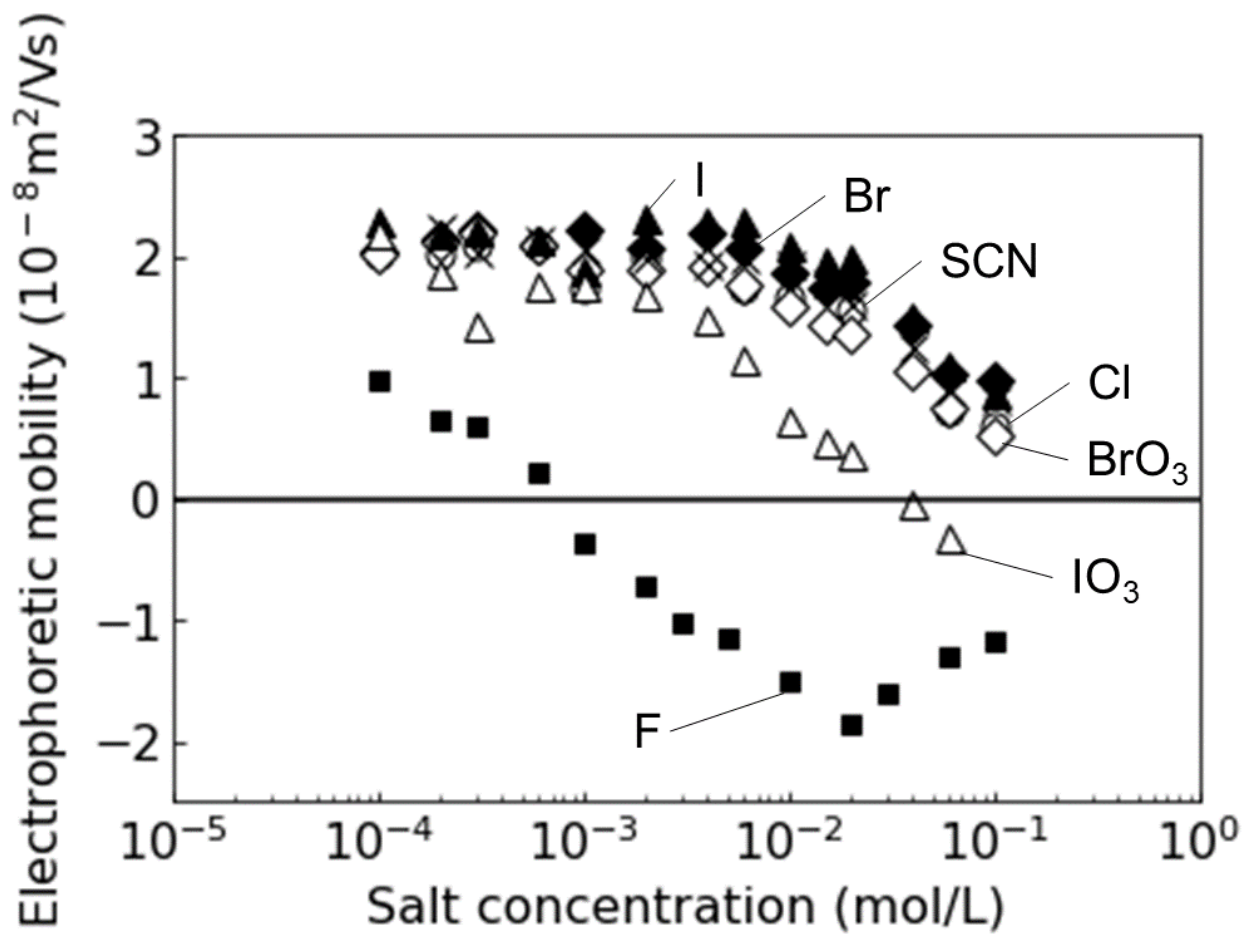
435 **allophane are plotted against the Gibbs free energy of hydration of anions ΔhydG (●). (b) The CCCs**

436 **obtained from the literature for the positively charged hydrophobic latex are shown (○, □). (c) The**

437 **CCCs and CSCs obtained from the literature for the positively charged hydrophilic latex are shown**
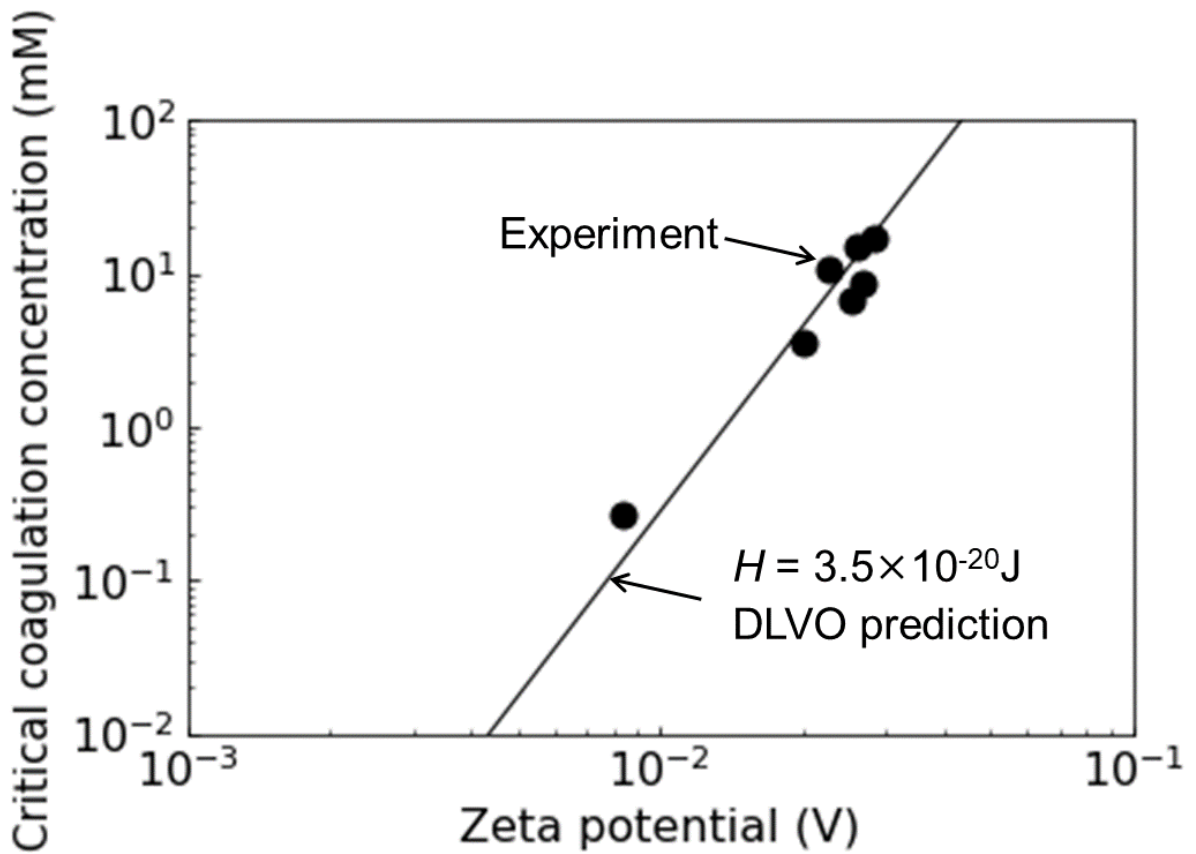
438 **(■,▲). The lines are drawn to guide the eyes only.**

439

440

441 **Fig. 5. Electrophoretic mobility of allophane as a function of the concentration of various monovalent**

442 **sodium salts of different anions. The particle concentration was 6 mg/L and the pH was fixed at 5.**

443

444

Fig. 6. Comparison between experimental CCC (filled circle) and the prediction by DLVO theory (line)

445

with $H = 3.5 \times 10^{-20}$ J, where H is the Hamaker constant for allophane-allophane in water. The

446

experimental CCC is plotted against zeta potential obtained from EPM measurements.

447

448